Available online at www.sciencedirect.com

ScienceDirect

Biochimica et Biophysica Acta 1778 (2008) 983–996

Biochimica et Biophysica Acta BBA

www.elsevier.com/locate/bbamem

Binding of LL-37 to model biomembranes: Insight into target *vs* host cell recognition

Rohit Sood [a], Yegor Domanov [a], Milla Pietiäinen [b], Vesa P. Kontinen [b], Paavo K.J. Kinnunen [a,*]

[a] *Helsinki Biophysics and Biomembrane Group, Medical Biochemistry, Institute of Biomedicine, P.O. Box 63 (Haartmaninkatu 8), FIN-00014 University of Helsinki, Finland*

[b] *Infection Pathogenesis Laboratory, Department of Viral Diseases and Immunology, National Public Health Institute, Mannerheimintie 166, FIN-00300 Helsinki, Finland*

Received 17 August 2007; received in revised form 20 November 2007; accepted 26 November 2007
Available online 14 December 2007

Abstract

Pursuing the molecular mechanisms of the concentration dependent cytotoxic and hemolytic effects of the human antimicrobial peptide LL-37 on cells, we investigated the interactions of this peptide with lipids using different model membranes, together with fluorescence spectroscopy for the Trp-containing mutant LL-37(F27W). Minimum concentrations inhibiting bacterial growth and lipid interactions assessed by dynamic light scattering and monolayer penetration revealed the mutant to retain the characteristics of native LL-37. Although both LL-37 and the mutant intercalated effectively into zwitterionic phosphatidylcholine membranes the presence of acidic phospholipids caused augmented membrane binding. Interestingly, strongly attenuated intercalation of LL-37 into membranes containing both cholesterol and sphingomyelin (both at $X=0.3$) was observed. Accordingly, the distinction between target and host cells by LL-37 is likely to derive from *i)* acidic phospholipids causing enhanced association with the former cells as well as *ii)* from attenuated interactions with the outer surface of the plasma membrane of the peptide secreting host, imposed by its high content of cholesterol and sphingomyelin. Our results further suggest that LL-37 may exert its antimicrobial effects by compromising the membrane barrier properties of the target microbes by a mechanism involving cytotoxic oligomers, similarly to other peptides forming amyloid-like fibers in the presence of acidic phospholipids.

Keywords: LL-37(F27W); Fluorescence spectroscopy; Acidic phospholipid; Phase separation; Cytotoxic oligomer; Amyloid-like fiber

Abbreviations: AMPs, antimicrobial peptides; Chol, cholesterol; CD, circular dichroism; DPPC, 1,2-dipalmitoyl-*sn*-glycero-3-phosphocholine; DPPE, 1,2-dipalmitoyl-*sn*-glycero-3-phosphoethanolamine; DPPG, 1,2-dipalmitoyl-*sn*-glycero-3-[phospho-*rac*-(1-glycerol)]; DPPDns, 1,2-dipalmitoyl-*sn*-glycero-3-phosphoethanolamino *N*-(5-dimethylaminonaphthalene-1-sulfonyl)triethylammonium salt; ET, energy transfer efficiencies; EDTA, ethylenediaminetetraacetic acid; FRET, fluorescence resonance energy transfer; K_{SV}, Stern–Volmer quenching constant; k_q, bimolecular quenching constant; K_d, apparent dissociation constant; LL-37, native LL-37; LL-37(F27W) with Phe27 replaced by Trp; LUV, large unilamellar vesicles; L/P, lipid to peptide ratio; LB, Luria–Bertani; MIC, minimal inhibitory concentration; NBD-PC, 1-oleoyl-2-[6-[7-nitro-2-1,3-benzoxadiazol-4-yl)amino]hexanoyl]-*sn*-glycero-3-phosphocholine; POPG, 1-palmitoyl-2-oleoyl-*sn*-glycero-3-phospho-rac-glycerol; POPS, 1-palmitoyl-2-oleoyl-*sn*-glycero-3-phospho-L-serine; (6,7)-Br_2-PC, 1-palmitoyl-2-(6,7-dibromostearoyl)phosphocholine; (9,10)-Br_2-PC, 1-palmitoyl-2-(9,10-dibromostearoyl)phosphocholine; (11,12)-Br_2-PC,-palmitoyl-2-(11,12-dibromostearoyl)phosphocholine; PC, phosphatidylcholine; PG, phosphatidylglycerol; PS, phosphatidylserine; P/L, peptide to lipid ratio; Q, quencher; RT, room temperature; Spm, sphingomyelin; SLBs, supported lipid bilayers; SOPC, 1-stearoyl-2-oleoyl-*sn*-glycero-3-phosphocholine; λ_{max}, fluorescence emission maximum; τ_f, fluorescence lifetime; ζ, zeta potential

* Corresponding author. Fax: +358 9 191 25444.
E-mail address: Paavo.Kinnunen@Helsinki.Fi (P.K.J. Kinnunen).

0005-2736/$ - see front matter © 2007 Elsevier B.V. All rights reserved.
doi:10.1016/j.bbamem.2007.11.016

1. Introduction

A variety of antimicrobial peptides (AMPs) constitute in the human body its first line of defense against microorganisms, including bacteria, fungi, and enveloped viruses [1–3]. These peptides have recently gained increasing interest because of their potential for treating infections by bacteria resistant to conventional antibiotics. Cathelicidins constitute a group of structurally diverse AMPs found only in mammals [4–7], and derived their name because of the similarity of their conserved N-terminal proregions to cathelin [8–10], a porcine leukocyte inhibitor of cathepsin L [3]. So far the only known human cathelicidin is LL-37 [11], which was identified as a putative AMP in a cDNA clone isolated from a human bone marrow library [4]. The mature LL-37 peptide (LLGDFFRKSKEKIGKEFKRIVQRIKDFLRNLVPRTES) was first isolated from granulocytes [12] and is also expressed in mast cells, neutrophils, as well as epithelial tissues, including skin, salivary glands, lung, urogenital and gastrointestinal tract. It is secreted into wounds, sweat, and airway surface fluids and is considered to play an important role against both local infections and systemic invasion of pathogens at sites of inflammation and damaged skin [13]. LL-37 is not as selective as some other α-helical, amphipathic AMPs, with MICs ranging from 1 to 10 μM for a variety of Gram-positive and Gram-negative bacteria, with eukaryotic cytotoxicity *in vitro* observed at 13–25 μM [14–16]. The antimicrobial activity of LL-37 has been confirmed also *in vivo* [17]. Intriguingly, in addition to its antimicrobial activity and stimulation of the innate immune system, LL-37 has been shown to be involved also in reproduction [18] and differentiation [19].

Recent studies on LL-37 have been mainly focused on its antimicrobial and cytotoxic activities and factors, which can inhibit its latter activity, such as truncation [20], and the presence of serum [21], or plasma [22]. LL-37 binds human plasma apolipoprotein A-I, which may act as a scavenger for this peptide [23]. It also associates with both plasma low density and very low density lipoproteins [22]. LL-37 is the first amphipathic α-helical AMP isolated from human, with 16 charged residues and a net charge of +6 at neutral pH [24]. Recent studies have shown that the amphipathic helix of LL-37 lies parallel to the membrane surface [21]. Neville et al. [25] observed lipid headgroup discrimination by LL-37. More specifically, LL-37 in low concentrations penetrates parallel to the plane into dipalmitoylphosphatiglycerol monolayers and resides in the phospholipid headgroup region. However, dipalmitoyl-phosphocholine and -phosphoethanolamine monolayers remained virtually unaffected. Oren et al. using fluorescence spectroscopy [21] and Henzler-Wildman et al. using solid state nuclear magnetic resonance and differential scanning calorimetery (DSC) [26] came to the conclusion that LL-37 forms "carpets" on the surface of both zwitterionic PC and negatively charged vesicles containing phosphatidylserine. NMR and DSC experiments revealed that LL-37 induces positive curvature strain but does not break membrane into smaller fragments or micelles [26–28]. More detailed understanding of the LL-37-lipid interactions, including structural changes that occur within the phospholipid bilayer, could aid the rational design of novel antibiotics.

In the present study we characterized the interactions of LL-37 with model biomembranes using Langmuir balance, dynamic light scattering, and circular dichroism. In order to employ fluorescence spectroscopy we constructed a mutant LL-37(F27W) with Phe27 replaced by Trp.

2. Experimental

2.1. Materials and methods

Hepes, EDTA, acryl amide, and Congo red were from Sigma. 1-Stearoyl-2-oleoyl-*sn*-glycero-3-phosphocholine (SOPC), 1-palmitoyl-2-oleoyl-*sn*-glycero-3-phospho-*rac*-glycerol (POPG), 1-palmitoyl-2-oleoyl-*sn*-glycero-3-phosphoserine (POPS), 1-palmitoyl-2-(6,7-dibromostearoyl)-*sn*-glycero-3-phosphocholine [(6,7)-Br_2-PC], 1-palmitoyl-2-(9,10-dibromostearoyl)-*sn*-glycero-3-phosphocholine [(9,10)-Br_2-PC], 1-palmitoyl-2-(11,12-dibromostearoyl)-*sn*-glycero-3-phosphocholine [(11,12)-Br_2-PC], 2-decanoyl-1-{*O*-[11-(4,4-difluoro-5,7-dimethyl-4-bora-3a,4a-diaza-sindacene-3-ropionyl)amino]undecyl}-*sn*-glycero-3-phosphol-choline (Bodipy-PC), sphingomyelin, and cholesterol were from Avanti Polar Lipids (Alabaster, AL). 1,2-Dipalmitoyl-*sn*-glycero-3-phosphoethanol amino *N*-(5-dimethylaminonaphthalene-1-sulfonyl), triethylammonium salt (DPPDns) and 1-oleoyl-2-{6-[(7-nitro-2-1,3-benzoxadiazol-4-yl)amino]hexanoyl}-*sn*-glycero-3-phosphocholine (NBD-PC) were from Molecular Probes (Eugene, OR). The purity of lipids was checked by thin-layer chromatography on silicic acid coated plates (Merck, Darmstadt, Germany) developed with a chloroform/methanol/water mixture (65:25:4, v/v/v). Examination of the plates after iodine staining, and when appropriate, upon UV illumination revealed no impurities. The concentrations of the lipids were determined gravimetrically with a high precision electrobalance (Cahn, Cerritos, CA) and lipid stock solutions were made in chloroform. Concentrations of fluorescent lipids DPPDns and NBD-PC were determined spectrophotometrically using their molar absorptivities of 21,000 (in CH_3OH) and 19,000 M^{-1} cm^{-1} (in C_2H_5OH) at 463 and 465, respectively. Large unilamellar vesicles (LUVs, with diameters between 111 and 117 nm) were prepared by extrusion (for cholesterol/sphingomyelin mixtures at 50 °C) through a 100 nm pore size (Millipore, Bedford, MA) filters essentially as described previously [29]. LL-37 and its F27W mutant were synthesized by Synpep (Dublin, CA) and their purities (>98%) verified by HPLC and mass spectrometry. All other chemicals were of analytical grade and from standard sources. Unless otherwise indicated the experiments were conducted using 5 mM Hepes, 0.1 mM ethylenediaminetetraacetic acid (EDTA), pH 7.0 buffer.

2.2. Antimicrobial activity of LL-37 and LL-37(F27W)

Bacillus subtilis strain 168 and *Staphylococcus aureus* strain Newman were used to determine minimal inhibitory concentrations (MIC) for LL-37 and LL-37(F27W). *B. subtilis* was grown in Luria–Bertani (LB) and modified Spizizen's minimal salts media (BFA, Anagnostopoulos and Spizizen, 1961), and *S. aureus* in BHI medium in shake flasks at 37 °C with vigorous shaking up to cell densities yielding $OD_{600}=1$. Approximately 10^5 cells of these cultures were used to inoculate 150 μl of growth media in honeycomb two plate wells for the determination of MIC values by plate reader (Bioscreen C Microbiology, Growth Curves Ltd, UK). The peptides were added to each well in two-fold dilution series from 0.5 μM to 16 μM, with three separate measurements for each peptide concentration. The MIC was the lowest concentration at which no bacterial growth was detected.

2.3. Circular dichroic (CD) spectra

UV-CD spectra from 250 to 190 nm were recorded with a CD spectrophotometer (Olis RSF 1000F, On-line Instrument Systems Inc., Bogart, GA) with cuvette temperature maintained at 25 °C with a circulating water bath. A 1-mm path length quartz cell was used with final concentrations of 20 μM and 3 mM of peptide and liposomes, respectively, in buffer. Interference by circular differential scattering by liposomes was eliminated by subtracting CD spectra for liposomes from those recorded in the presence of peptide. Data are shown as mean residue molar ellipticity (deg cm^2 $dmol^{-1}$) and represent the averages of seven scans. The

percentage of helical content was estimated from the molar ellipticity at 222 nm (θ_{222}) [30].

2.4. Monolayer penetration

Insertion of LL-37 and LL-37(F27W) into lipid monolayers residing on an air/buffer interface was measured using a miniaturized Langmuir tensiometer (DeltaPi, Kibron Inc., Helsinki, Finland) with magnetically stirred circular Teflon wells, essentially as described previously [31]. The indicated lipids (approximately 1 mg/ml, in chloroform) were spread onto the air/buffer interface. All measurements were made in triplicate and performed at ambient temperature (~+24 °C).

2.5. Dynamic light scattering and measurement of zeta potential

The impact of LL-37 and LL-37(F27W) on the apparent size distribution of LUVs was determined by DLS using photon correlation spectroscopy at a scattering angle of 173° (Zetasizer Nano ZS, Malvern Instruments Ltd., UK). Lipid concentration was 20 μM with the indicated concentrations of peptide added and DLS performed after a 30 min incubation at 25 °C. Hydrodynamic diameters (d_Z, nm) were calculated from the diffusion coefficient (D) using the Stokes–Einstein equation

$$d_Z = kT/3\pi\eta D \quad (1)$$

where k is the Boltzmann constant, T the absolute temperature, and η the viscosity of the solvent. Each data point represents the mean of three independent measurements.

The zeta potential (ζ) of the liposomes was determined by laser Doppler electrophoresis with the above instrument using dedicated disposable cells. From the obtained electrophoretic mobility, the zeta potential was calculated using the Smoluchowski equation

$$\zeta = 4\pi\eta u/\varepsilon \quad (2)$$

where u is the electrophoretic mobility, η the viscosity of the solvent, and ε its dielectric constant. The lipid concentration used was 250 μM, chosen so as to obtain a high enough count rate at 25 °C. Each data point represents the mean of three independent measurements with SD.

2.6. Microscopy of amyloid-like fibrils

Amyloid-like fiber formation was assessed by adding LL-37 or LL-37(F27W) to the buffer containing SOPC, SOPC/POPG, or SOPC/POPS ($X_{POPG}=X_{POPS}=0.2$) LUVs to yield final peptide and lipid concentrations of 3 μM and 120 μM, respectively. The samples were observed by bright field microscopy. For polarized microscopy, the fibers were incubated for 30 min with 10 μM Congo red and their resulting birefringence was observed using crossed polarizers in the excitation and emission paths. When indicated, trace amounts ($X=0.02$) of the fluorescent lipid NBD-PC was additionally included in the liposomes, and fibers were formed as described above, imaging their fluorescence with the confocal microscope with excitation at 488 nm [32].

2.7. Interactions with supported planar bilayers (SPB)

Supported bilayers were prepared as described previously [33]. In brief, appropriate amounts of lipid stock solutions were mixed in chloroform to obtain the desired compositions, with the fluorescent lipid derivative Bodipy-PC constituting $X=0.005$ of total lipid. The solvent was removed under a stream of nitrogen and the lipid residue subsequently maintained under reduced pressure for at least 1 h. The dry lipids were hydrated with buffer at RT and the resulting dispersions extruded through a 50 nm pore size polycarbonate filter (Millipore, Bedford, MA). Bilayers were formed by liposome fusion on glass cover slips in the presence of calcium [33].

2.8. Fluorescence spectra and lifetime measurements

All fluorescence measurements were performed in one cm path length quartz cuvettes. LUVs were added to a solution of LL-37(F27W) (3 μM final concentration in buffer) maintained at 25 °C in a total volume of 2 ml. After equilibration for one h fluorescence spectra were measured with a Perkin Elmer LS 50B spectrometer with both emission and excitation bandpasses set at 5 nm. The tryptophan residue of LL-37(F27W) was excited at 280 nm and emission spectra were recorded from 290 to 450 nm, averaging five scans. Spectra were recorded as a function of lipid/peptide (L/P) molar ratio and corrected for the contribution of light scattering measured in the presence of vesicles only. Blue shifts were calculated as the differences in center of mass of the emission spectra. S.D. in the blue shift was less than 0.5 nm. Fluorescence lifetimes were measured and data analyzed essentially as discussed previously [34].

2.9. Quenching of Trp emission by acrylamide, dansyl, and brominated phophatidylcholines

To reduce the absorbance by acrylamide, excitation of Trp at 295 nm instead of 280 nm was used [35]. Aliquots of a 3.0 M solution of this water-soluble collisional quencher were added to a solution of the peptide in the absence or presence of liposomes at a peptide/lipid (P/L) molar ratio of 1:80. The values were corrected for scattering, the latter derived from acrylamide titration of a vesicle blank. The data were analyzed according to the Stern–Volmer equation [36].

$$F_0/F = 1 + K_{sv}[Q] = 1 + k_{q\tau 0}[Q] \quad (3)$$

where F_0 and F represent the fluorescence intensities in the absence and presence of the quencher (Q), respectively, and K_{sv} is the Stern–Volmer quenching constant. The latter reflects in this case the accessibility of Trp to acrylamide and is defined as

$$K_{sv} = k_q\tau_0 \quad (4)$$

where k_q is the bimolecular quenching constant and τ_0 is the lifetime of the fluorophore in the absence of quencher. As acrylamide is neutral it has no electrostatic interactions with the headgroups of the negatively charged phospholipids. On the premise that acrylamide does not significantly partition into the membrane bilayer [35], the value for K_{sv} can be considered to provide a measure of the bimolecular rate constant for collisional quenching of the Trp residue in contact to the aqueous phase. Accordingly, K_{sv} depends on the amount of free peptide in solution as well as the fraction of the peptide residing in the surface of the bilayer.

To utilize the resonance energy transfer in assessing the binding of LL-37 (F27W) to phospholipids a fluorescent lipid, DPPDns, ($X=0.03$) was incorporated into the liposomes as an acceptor. Small aliquots of 1 mM liposome solution were added to 3 μM LL-37(F27W) in a total volume of 2 ml buffer maintained at 25 °C. Trp was excited at 280 nm with excitation and emission bandpasses set at 7 nm. Energy transfer efficiencies were calculated using the equation

$$E = (1 - F/F_0) \quad (5)$$

where F_0 and F represent the fluorescence intensities at 350 nm in the absence and presence of acceptor, respectively.

Collisional quenching of Trp by brominated phospholipids (Br_2-PC) was utilized to assess its localization in bilayers. The indicated LUVs were added to a solution of LL-37 (F27W) to yield a final peptide concentration of 3 μM in buffer. After 1 h at 25 °C, emission spectra were recorded, averaging five scans. The differences in the quenching of Trp fluorescence by (6, 7)-, (9, 10)-, and (11, 12)-Br_2-PC were used to calculate the probability for location of W27 in the membrane using both the parallax method [37] and distribution analysis [38,39].

3. Results

3.1. Antimicrobial activities of LL-37 and LL-37(F27W)

In order to use Trp fluorescence in assessing the interactions of LL-37 with lipid membranes we constructed an LL-37

mutant, LL-37(F27W) with Phe27 replaced by Trp. The former residue was selected for substitution so as to introduce a minimal perturbation to the physicochemical characteristics of the peptide. In order to check the impact of this replacement we first compared the antimicrobial efficiencies of LL-37(F27W) and the native peptide. For *B. subtilis* MIC values of LL-37 and LL-37(F27W) were 2 and 4 μM in LB-medium, respectively, and one μM for both peptides in BFA-medium. In contrast *S. aureus* is highly resistant to LL-37 and no effect on its growth was detected up to 16 μM concentrations of either LL-37 or LL-37(F27W). Accordingly, we conclude the antimicrobial activity of LL-37 to be insignificantly affected by this substitution.

3.2. Secondary structure of LL-37 and LL-37(F27W)

LL-37 is in a random disordered state at micromolar concentrations in water yet undergoes a cooperative transition into an α-helix upon increasing its concentration [20]. CD spectra of LL-37(F27W) were recorded to check if the single amino acid substitution altered the secondary structure of the peptide. The characteristic double minima at 208 nm and 222 nm (Fig. 1) was observed for LL-37(F27 W) in buffer, revealing α-helical secondary structure, as reported for the native peptide [20]. In the presence of SOPC and SOPC/POPG (X_{POPG}=0.4) LUVs the calculated helical content increased to 13 and 22%, respectively.

3.3. Penetration of LL-37 and LL-37(F27W) into lipid monolayers

In keeping with their amino acid compositions both LL-37 and LL-37(F27W) were surface active and intercalated effectively into lipid monolayers, as illustrated for an SOPC/POPG film (X_{POPG}=0.2) at an initial pressure π_0=24.5 mN/m (Fig. 2, *panels A and B*). The extent of their penetration into the lipid films was indistinguishable as demonstrated by the similar values for $\Delta\pi$. However, the kinetics of binding were different and a slight decrease in π was observed for native LL-37 following the initial intercalation (Fig. 2, *panel A*), before reaching a plateau. This decrement was not observed for LL-37 (F27W). Irrespective of their overall net positive charge (+6) both LL-37 and LL-37(F27W) inserted equally effectively into both zwitterionic (SOPC) as well as negatively charged SOPC/POPG (X_{POPG}=0.2) and SOPC/POPS (X_{POPS}=0.2) monolayers. The values of packing pressure π_c abrogating the intercalation of LL-37(F27W) into monolayer were 44 (neat SOPC), and 47 mN/m (X_{POPG}=0.2 and X_{POPS}=0.2). For LL-37 these values were 44 (neat SOPC), 48 (X_{POPG}=0.2), and 41 mN/m (X_{POPS}=0.2). Interestingly, while cholesterol (X=0.1 or 0.3) and sphingomyelin (X=0.1 or 0.3) alone attenuated the intercalation of both LL-37 and LL-37 (F27W) into the monolayers, least efficient insertion was evident for monolayers containing both cholesterol and sphingomyelin (X_{Chol}=X_{Spm}=0.3, Fig. 2, *panels E and F*), with π_c=26 and 25 mN/m for LL-37 (F27W) and LL-37, respectively. This value is well below the equilibrium lateral pressure of approximately 30–35 mN/m estimated for biomembranes [40,41].

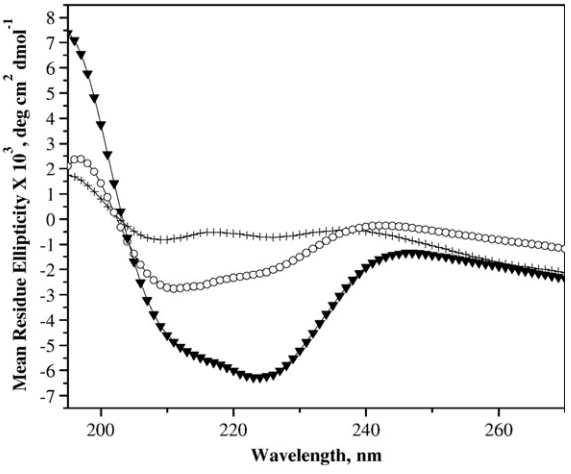

Fig. 1. Circular dichroic spectra of 5 μM LL-37(F27W) in buffer (+) and in the presence of SOPC/POPG, X_{POPG}=0 (○), 0.4 (▼) LUVs. Final lipid concentration was 3 mM, corresponding to P/L=1/600. The temperature was maintained at 20 °C with a circulating water bath.

3.4. Changes in apparent liposome size and zeta potential induced by LL-37 and LL-37(F27W)

Binding of LL-37 and LL-37(F27W) to liposomes was also assessed by dynamic light scattering. Apparent average hydrodynamic diameters d_Z of 92, 91, 93, and 98 nm were measured for SOPC, SOPC/POPG (X_{POPG}=0.2), SOPC/Chol (X=0.1), and SOPC/Chol/Spm (X_{Chol}=X_{Spm}=0.3) liposomes, respectively. Upon addition of LL-37(F27W) to SOPC and SOPC/Chol (X_{Chol}=0.1) liposomes increase in d_Z was observed until P/L=0.005 and P/L=0.010 (Fig. 3, *panel D*), respectively. Upon further addition of the peptide d_Z decreases and becomes constant above P/L=0.010 and 0.0125 for SOPC and SOPC/Chol (X_{Chol}=0.1) liposomes, respectively. Addition of LL-37 and LL-37(F27W) to liposomes with X_{POPG}=0.2 caused a progressive decrease in d_Z at all P/L ratios (Fig. 3, *panels C & D*). In contrast, an increase in d_Z was evident for SOPC/Chol/Spm (X_{Chol}=X_{Spm}=0.3) liposomes until P/L=0.025 (Fig. 3, *panels C & D*).

The values for the zeta potential ζ of SOPC, SOPC/Chol (X_{Chol}=0.1), SOPC/Chol/Spm (X_{Chol}=X_{Spm}=0.3) and SOPC/POPG (X_{POPG}=0.2) liposomes were −15, −17, −19 and −47 mV, respectively (Fig. 3, *panels A and B*). Both peptides increased ζ for zwitterionic as well as anionic liposomes and caused charge reversal for zwitterionic liposomes at P/L=0.01. Upon further addition of peptide (P/L>0.006) the values for ζ remained unaltered.

3.5. Formation of amyloid-like fibers

Microscopy experiments revealed that fibrous aggregates developed upon adding LL-37 or LL-37(F27W) to SOPC/POPG (X_{POPG}=0.2) liposomes (Fig. 4, *panel A*). There was no specificity with respect to the acidic phospholipid headgroup and similar fibers were observed for SOPC with X_{POPS}=0.2 (data not shown). Subsequent Congo red staining of these fibers did yield the light green birefringence characteristic for amyloid

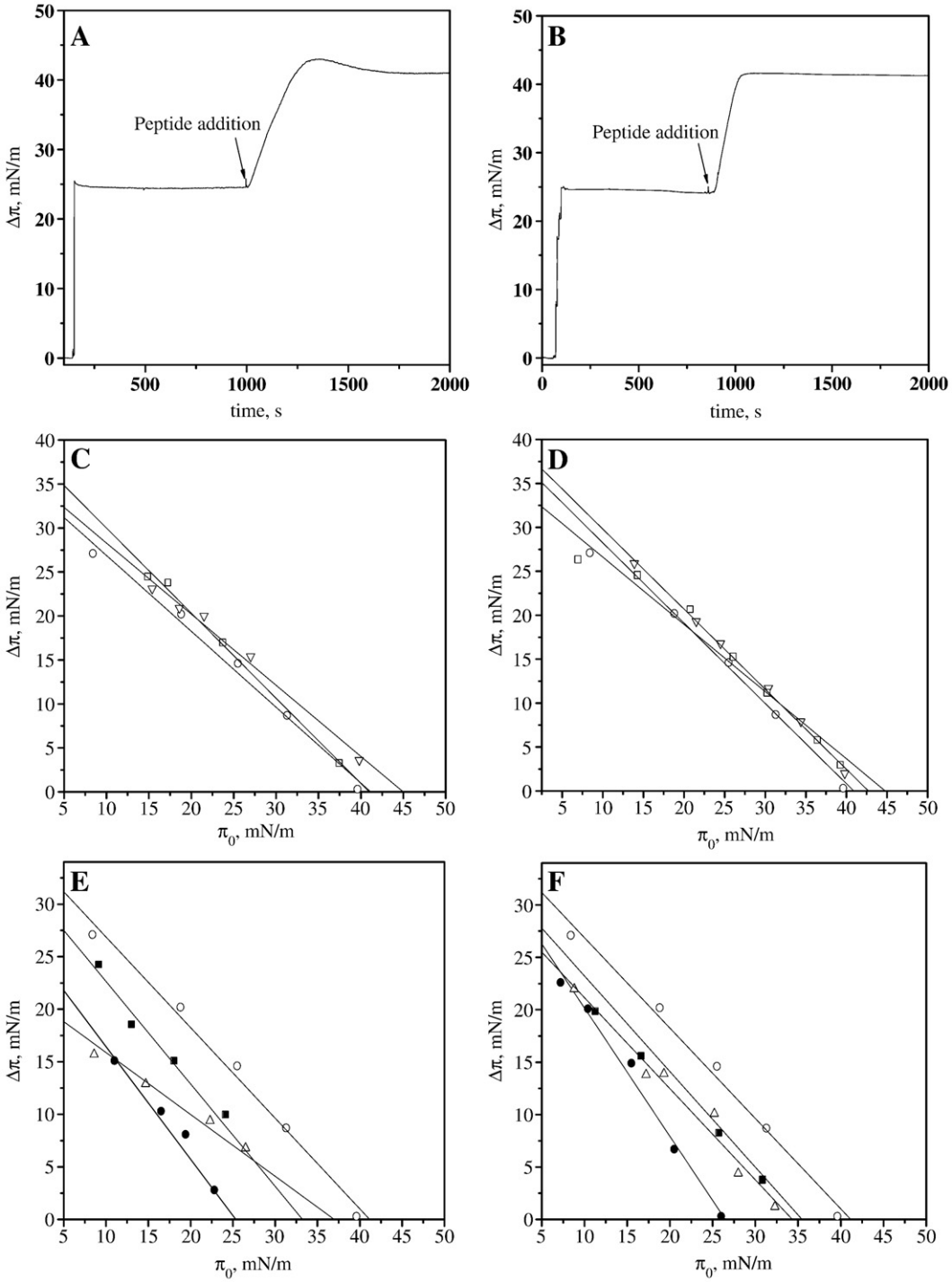

Fig. 2. Insertion of LL-37 and LL-37(F27W) into lipid monolayers. Increase in surface pressure is depicted as a function of time following the injection of LL-37 (*panel A)* and LL-37(F27W) (*panel B)* to yield a final concentration of 0.3 μM underneath a SOPC/POPG ($X_{POPG}=0.2$) monolayer at an initial surface pressures (π_0) of approximately 24.3 mN/m. Increments in surface pressure ($\Delta\pi$) as a function of the initial surface pressure (π_0) for monolayers of SOPC (○) alone and with $X_{POPG}=0.2$ (▽), $X_{POPS}=0.2$ (□), or with $X_{Chol}=0.3$ (Δ), $X_{Spm}=0.3$ (■), or $X_{Chol}=X_{Spm}=0.3$ (●) due to either 0.3 μM LL-37 (*panels C and E*) or LL-37(F27W) (*panels D and F*) injected at T ≈ 24 °C into the subphase.

(Fig. 4, *panel B*). These fibers became fluorescent when trace amount of NBD-PC was present in the liposomes (Fig. 4, *panel C*), thus revealing that the fibers incorporate phospholipids, as shown for fibers formed by the other cytotoxic or apoptotic proteins that we have studied [32,42,43].

3.6. Interactions with supported bilayers

Wild-type LL-37 caused significant perturbation of supported lipid bilayers (SLBs) containing acidic phospholipids (Fig. 5). Within the first 10 min a progressive vesiculation was

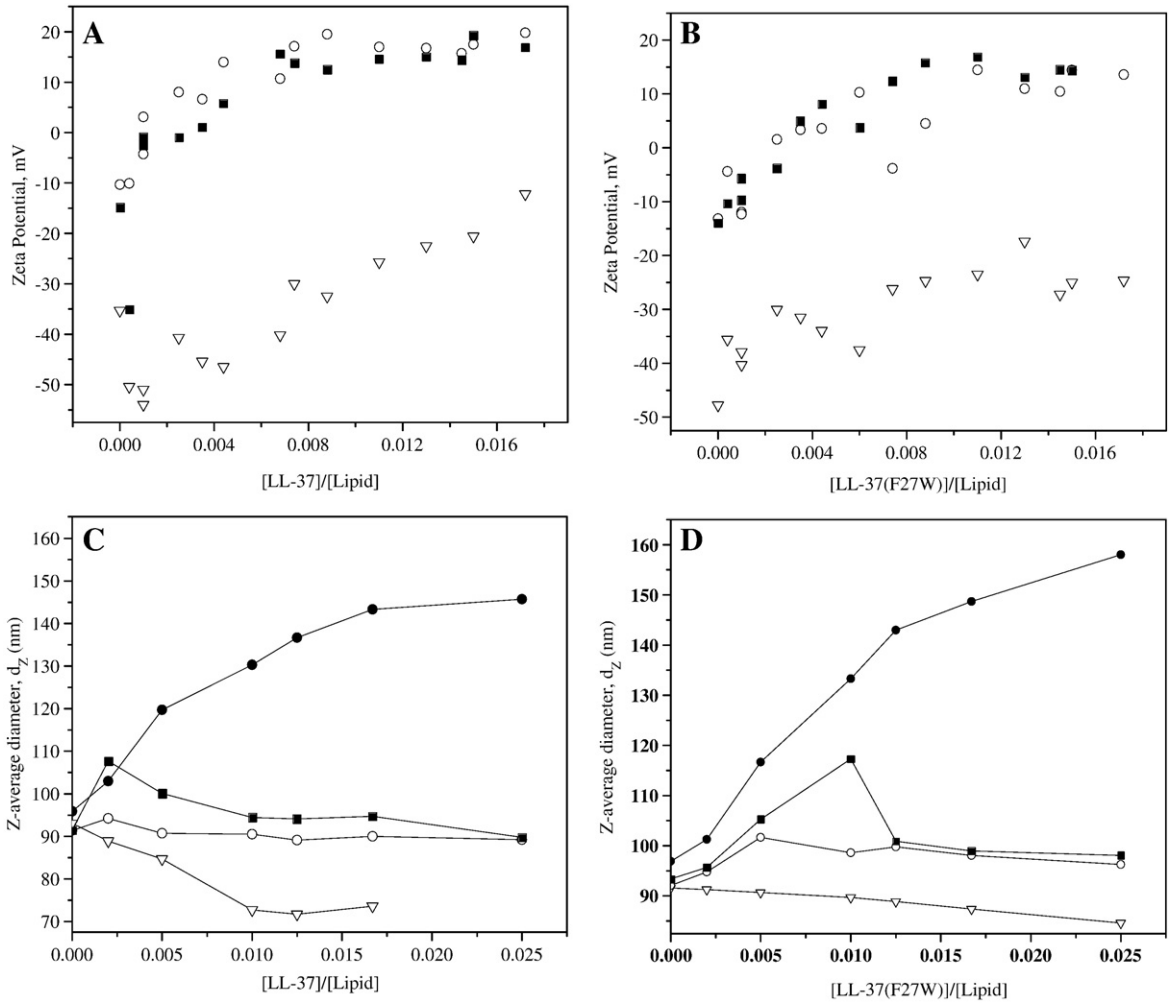

Fig. 3. Zeta potential (ζ) for liposomes composed of SOPC with $X_{POPG}=0$ (○), 0.2 (▽), $X_{Chol}=0.1$ (■), and SOPC with $X_{Chol}=X_{Spm}=0.3$ (●) at the indicated peptide/lipid ratios for LL-37 *(panel A)* and LL-37(F27W) *(panel B)*, respectively. The experiments were carried out at ambient temperature (approximately 24 °C) and each data point represents the mean of triplicate measurements. Also shown are apparent liposome sizes represented as the *Z*-average diameters for SOPC with $X_{POPG}=0$ (○), 0.2 (▽), $X_{Chol}=0.1$ (■), and with $X_{Chol}=X_{Spm}=0.3$ (●) at the indicated P/L ratios of LL-37 *(panel C)* and LL-37(F27W) *(panel D)*.

seen, with multilamellar and unilamellar vesicles of up to 1 μm in diameter emerging from the SLB. Subsequently, some of these vesicles detached from the surface. Longer incubation (for hours) led to further increase in the size of these vesicles as well as spreading of some of them on the SLB and formation of multibilayer structures. Notably, although the nominal peptide concentration in these experiments was low (0.4 μM) this corresponds to L/P ratio of ~2:1, when taking into account the total amount of lipid in the chamber (420 pmol). Changes induced by LL-37(F27 W) were indistinguishable from those due to the wild type peptide (data not shown).

3.7. Lipid induced changes in the fluorescence of LL-37(F27W)

We then studied the lipid association of LL-37(F27W) using Trp fluorescence. In aqueous solutions emission maximum λ_{max} for LL-37(F27W) was observed at 350 nm, characteristic of Trp in a polar environment. The fluorescence of LL-37 (F27 W) was markedly altered upon the addition of liposomes with λ_{max} shifting to shorter wavelengths (≈340 nm) together with enhanced emission *I*, typically for Trp accommodated in a hydrophobic environment and in keeping with W27 residing in the hydrocarbon region of the lipid bilayer. However, for liposomes with $X_{Chol}=X_{Spm}=0.3$ a shift of only approx. = 1.5 nm in λ_{max} was observed (data not shown).

Fluorescence of Trp of LL-37(F27W) as a function of L/P ratio did yield conventional binding curves (Fig. 6, *panel A*), with significant differences between the different liposome compositions. Yet, regardless of their composition the values for $\Delta\lambda_{max}$ measured in the presence of liposomes reached a plateau at L/P ≈ 40. For neat SOPC liposomes and at L/P <20 the value for $\Delta\lambda_{max}$ was approx. 10 nm, increasing less steeply with L/P. The blue shift saturated at L/P = 40 and was maximally approximately 12 nm. In the presence of SOPC/POPG liposomes there was a sharp increase in $\Delta\lambda_{max}$ to 13 nm at L/P <20. This effect was most pronounced with $X_{POPG}=0.4$, with blue shifts of about 12.5, 13.0, and 14.0 nm at $X_{POPG}=0.1$, 0.2, and 0.4, respectively. Identical changes in Trp emission were seen for liposomes containing POPS instead of POPG. Accordingly, binding of LL-37(F27W) to liposomes is not specific to the headgroup of the acidic

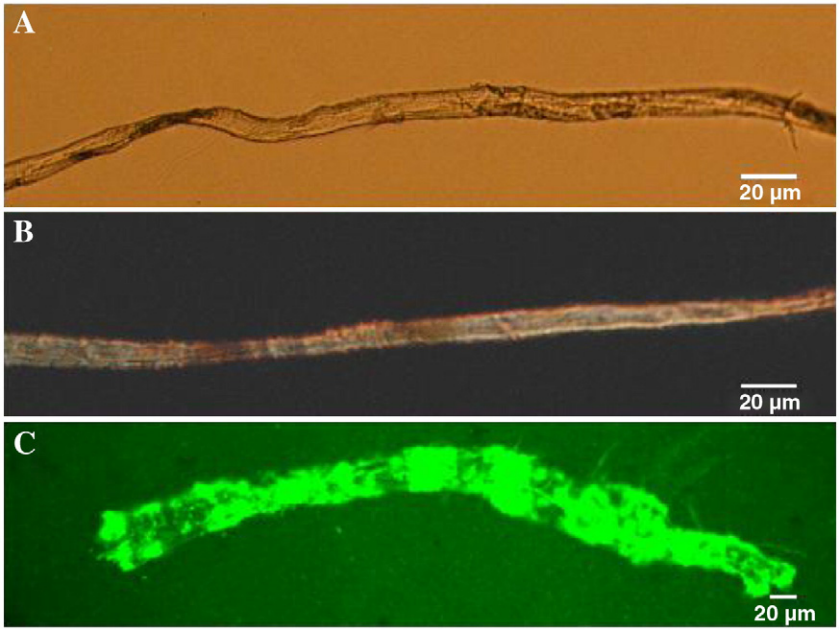

Fig. 4. *Panel A:* Bright field microscopy image of a fiber formed by LL-37(F27W) after mixing with SOPC/POPG (X_{POPG}=0.2) liposomes at ambient temperature (approximately 24 °C). The final concentrations of the phospholipid and peptide were 100 μM and 3 μM. *Panel B*: The fiber formed by LL-37(F27W) but after staining with Congo red (final concentration of 10 μM). *Panel C:* Incorporation of the fluorescent phospholipid analogue NBD-PC into the fiber. The latter was formed as described above except that a trace amount (X=0.02) of NBD-PC was additionally included in the SOPC/POPG liposomes.

phospholipid, confirming results from DLS and monolayer measurements. Cholesterol at X_{Chol}=0.1 slightly attenuated the changes in $\Delta\lambda_{max}$, including the level of plateau. Upon increasing the content of cholesterol (X_{Chol}=0.3) and further including also sphingomyelin (X_{Chol}=X_{Spm}=0.3) reduced dramatically the shift in λ_{max}. Accordingly, at L/P=40 blue shifts of 10.0, 8.0, and 1.5 nm were evident for SOPC vesicles with X_{Chol}=0.1, X_{Chol}=X_{Spm}=0.1, and X_{Chol}=X_{Spm}=0.3, respectively, suggesting that for the latter composition the membrane association and penetration of LL-37(F27W) into the lipid bilayer were strongly attenuated.

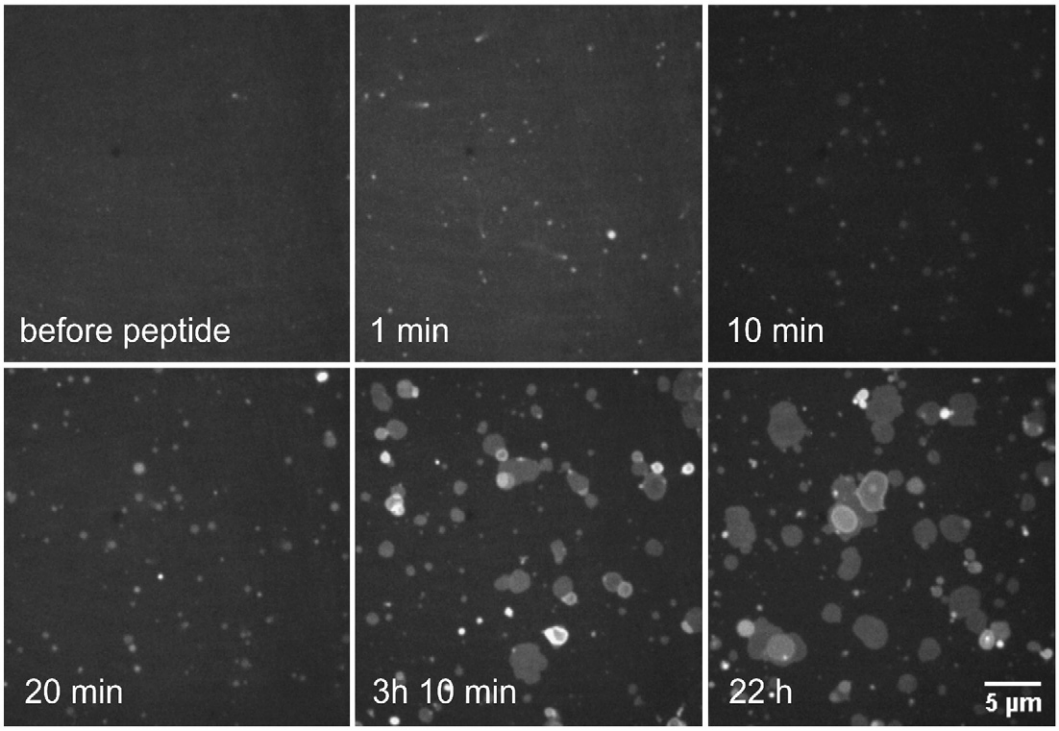

Fig. 5. Time course of supported lipid bilayer perturbation by wild-type LL-37. Time after the addition of LL-37 is indicated in the panels. Nominal peptide concentration in the chamber was 0.4 μM in 20 mM Hepes, 0.1 mM EDTA, pH 7.0. Lipid composition of the bilayer was SOPC/POPG/Bodipy-PC, (X_{POPG}=0.2, X_{Bodipy}=0.005). Panels corresponding to 0–20 min show the same patch of the bilayer.

Quantitative analysis of the lipid titration curves and the values of the shift in λ_{max} as a result of membrane incorporation yield the apparent equilibrium dissociation constant K_d for the different lipid compositions (Table 1). K_d decreases for negatively charged liposomes compared to zwitterionic membranes, indicating a higher affinity of LL-37(F27W) towards former. Partition coefficients for vesicles with $X_{Chol}=X_{Spm}=0.3$ could not be evaluated due to the flatness of the curve (Fig. 6, *panel A*). We also studied the variation of *I* as a function of L/P ratio (Fig. 6, *panel B*). A decrease in *I* of Trp was observed at L/P=5 for all the lipid compositions studied. At L/P>5 the values for *I* increased, with the largest increment observed at L/P=60 with further addition of LUVs having an insignificant effect. At L/P=5 the decrease in *I* is most pronounced for the zwitterionic SOPC liposomes. As the content of POPG increased, decrease in *I* was evident at L/P=5 (Fig. 6, *panel B*) and after this molar ratio a pronounced and progressive increase in *I* was seen. Similar behavior was observed with liposomes containing POPS ($X_{POPS}=0.2$). Minor effect was evident at $X_{POPG}=0.4$

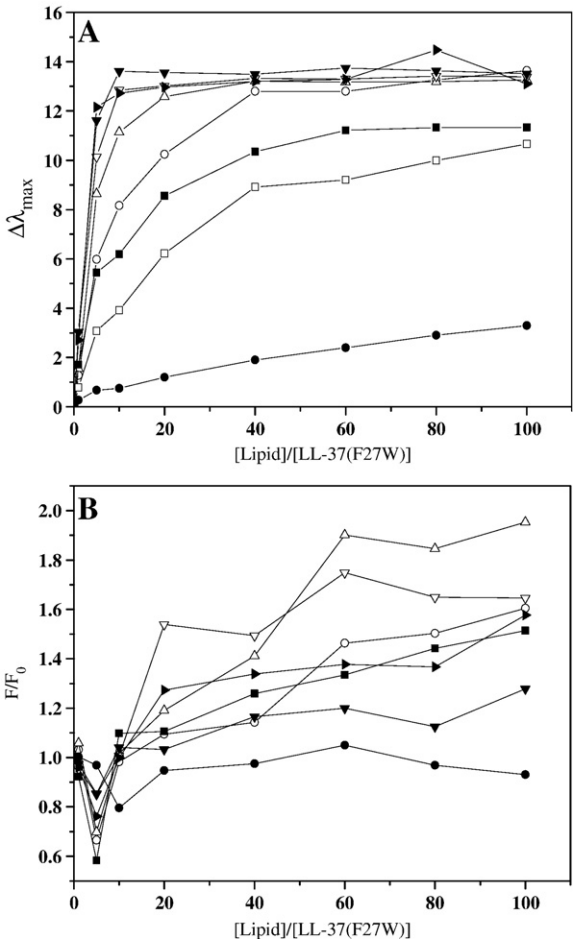

Fig. 6. *Panel A*: Blue shift in the Trp emission maxima in the presence of liposomes composed of SOPC with $X_{POPG}=0$ (○), 0.1 (Δ), 0.2 (▽), 0.4 (▼), $X_{POPS}=0.2$ (▶), $X_{Chol}=0.1$ (■), SOPC with $X_{Chol}=X_{Spm}=0.1$ (□) and SOPC with $X_{Chol}=X_{Spm}=0.3$ (●) as a function of lipid/peptide ratio. *Panel B*: Changes in fluorescence intensity as a function of lipid/peptide ratio. Symbols are identical to those in panel A. The final concentration of LL-37(F27W) in all experiments was 3 μM in a total volume of 2 mL of 5 mM Hepes, 0.1 mM EDTA, pH=7.0. The temperature was maintained at 25 °C with a circulating water bath.

Table 1
Values for the apparent dissociation constant (K_d, μM) and the corresponding chi2 (χ^2) for the binding of LL-37(F27W) to the indicated liposomes and calculated by fitting the data to the Langmuir isotherm

Liposomes	K_d, μM	χ^2
SOPC	23.8	0.11
$X_{POPG}=0.1$	0.51	0.07
$X_{POPG}=0.2$	0.40	0.05
$X_{POPS}=0.2$	0.28	0.27
$X_{POPG}=0.4$	0.12	0.04

where *I* first decreased at L/P=5, followed by an increase. The increment in *I* was much smaller compared to $X_{POPG}=0.1$, 0.2, and $X_{POPS}=0.2$ for which a progressive enhancement of intensity was seen at L/P>10. In the presence of liposomes containing both cholesterol and sphingomyelin at $X=0.3$ the fluorescence intensity decreased slightly at all L/P ratios, in keeping with the small change in the τ_{av} (see below).

3.8. Time resolved Trp fluorescence

Not only the spectral features but also the fluorescence lifetimes (τ_f) of Trp depend on its microenvironment [44]. Representative fluorescence intensity decays for LL-37(F27W) in buffer and in the presence of SOPC/POPG ($X_{POPG}=0.2$) LUVs with their biexponential fitting and the statistical parameters used to check the quality of the fit are illustrated (Fig. 7, *panels A & B and C & D,* respectively). The average fluorescence lifetimes (τ_{av}) are plotted as a function of L/P ratio (Fig. 7, *panel C*). The variation in τ_{av} parallels the changes in steady state emission intensity *I* at all L/P ratios. In brief, τ_{av} decreased up to L/P=5 while above this ratio its values increased and leveled off at approximately L/P=40. At L/P=5 the decrease in τ_{av} is significant for SOPC liposomes, however, as X_{POPG} increases, decrease in τ_{av} diminished (Fig. 7, *panel E*). Above L/P=5 a progressive increment in τ_{av} was evident. Similar behavior was seen for liposomes containing POPS ($X_{POPS}=0.2$). As observed in steady state measurements, behavior with $X_{POPG}=0.4$ was different and was in accordance with the changes in *I*. Accordingly, τ_{av} first decreased at L/P=5 and then increased, however, the increment in τ_{av} was much smaller compared to $X_{POPG}=0.1$, 0.2, and $X_{POPS}=0.2$. In the presence of SOPC LUVs $\tau_{av}=4.2$ ns at L/P=40 whereas values of 5.4 and 6.0 ns were observed with $X_{POPG}=0.1$, and 0.2, respectively, in keeping with the augmented interaction of the peptide with negatively charged lipids. The decrease in τ_{av} observed at L/P≤10 for neat SOPC and SOPC containing acidic phospholipids is somewhat unexpected since due to fast deactivation processes Trp lifetimes are shorter in polar solvents [45]. The shortening of τ_{av} could be caused by proximity of W27 and R23 when in a helical conformation, the latter residue having p*K*a of 12.48, and thus being positively charged at physiological pH, leading to cation–π interaction [46,47]. At L/P≥20 values of τ_{av} in the presence of liposomes were longer compared to values measured in buffer, indicating Trp to reside in a hydrophobic region of the bilayer. For liposomes containing cholesterol and sphingomyelin τ_{av} decreased at all L/P ratios with $\tau_{av}=3.3$ ns being measured for

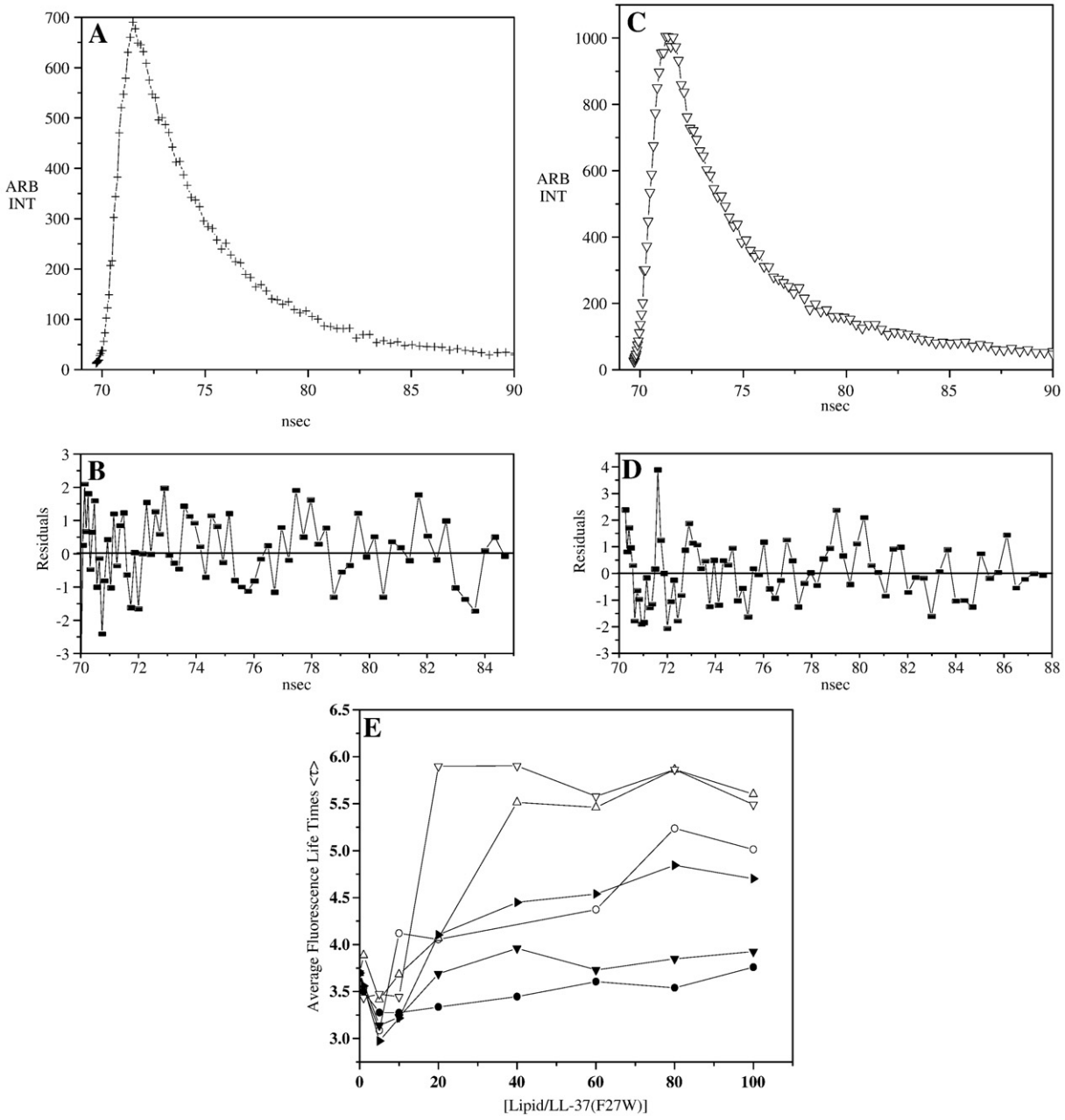

Fig. 7. Time resolved fluorescence intensity decay for LL-37(F27W) in buffer (+) at 25 °C (*Panel A)* and its weighed residuals (*panel B)*. The concentration of LL-37 (F27W) was 3 μM in a total volume of 2 mL of 5 mM Hepes, 0.1 mM EDTA, pH=7.0. Excitation wavelength was 295 nm with emission monitored at 350 nm. For comparison intensity decay recorded in the presence of SOPC/POPG (X_{POPG}=0.2) LUVs (L/P=100) with residuals are also illustrated (*panels C and D*, respectively). *Panel E*: Average fluorescence lifetimes (τ_{av}) of membrane bound LL-37(F27W) as a function of lipid/peptide ratio. The fluorescence lifetimes were calculated for liposomes composed of SOPC with X_{POPG}=0 (○), 0.1 (Δ), 0.2 (▽), 0.4 (▼), X_{POPS}=0.2 (▶), and SOPC with X_{Chol}=X_{Spm}=0.3 (●).

X_{Chol}=X_{Spm}=0.3 at L/P=40, in keeping with the least change in λ_{max} (Fig. 6, *panel A*) and *I* (Fig. 6, *panel B*), and revealing the fluorophore to be in a polar environment, in line with the observations on this composition being effective in restricting the penetration of the peptide into the bilayer.

3.9. Quenching of Trp by acrylamide and FRET measurements

To investigate the orientation of LL-37(F27W) in the membrane and lipid specificity of the peptide/liposome interaction we used acrylamide as a water-soluble collisional quencher of Trp. Stern–Volmer plots for Trp fluorescence demonstrated a concentration dependent decrease both in the absence and presence of liposomes without other effects on the spectra (data not shown). In buffer Stern–Volmer constant K_{sv} was 11.8 M^{-1}, revealing a direct access of the quencher to Trp. However, the values for K_{sv} decreased significantly in the presence of SOPC, SOPC/POPG, SOPC/POPS, and SOPC/Chol LUVs (Table 2), indicating that Trp become accommodated within the bilayer, the minor differences in K_{sv} suggesting similar and poor accessibility of acrylamide to Trp. Interestingly, as the molar concentration of both cholesterol and sphingomyelin in liposomes was

Table 2
The values of the Stern–Volmer quenching constant K_{sv} and the bimolecular quenching constant k_q ($\times 10^{-9}$ M^{-1} s^{-1}) for LL-37(F27W) at L/P=80 by acrylamide in buffer and in the presence of liposomes with the indicated compositions

Liposomes	K_{sv}	k_q
Buffer	11.8±0.2	3.10
SOPC	1.6±0.1	0.47
X_{POPG}=0.1	1.6±0.1	0.38
X_{POPG}=0.2	1.8±0.1	0.51
X_{POPS}=0.2	1.7±0.1	0.51
X_{POPG}=0.4	1.7±0.1	0.52
X_{Chol}=0.1	1.7±0.1	0.51
$X_{Chol/Spm}$=0.1	2.7±0.1	1.40
$X_{Chol/Spm}$=0.3	8.3±0.1	2.70

increased the accessibility of the quencher to Trp increased, as reflected in the increase of K_{sv} confirming these lipids at $X_{Chol}=X_{Spm}=0.3$ to be highly effective in reducing the membrane intercalation of LL-37(F27W).

Lipid binding of LL-37(F27W) was further assessed by resonance energy transfer (RET) from Trp to dansyl-labeled lipid (DPPDns) incorporated into liposomes. RET is demonstrated by the attenuated Trp emission recorded in the range of 290 to 450 nm in the presence of increasing concentrations of SOPC/POPG/DPPDns ($X_{POPG}=0.2$, $X_{DPPDns}=0.03$) liposomes (Fig. 8, *panel A*) in keeping with augmented membrane binding of LL-37 (F27W) in the presence of the negatively charged lipid (Fig. 8, *panel C*). In the presence of SOPC and SOPC/Chol/Spm/DPPDns ($X_{Chol}=X_{Spm}=0.3$, $X_{DPPDns}=0.03$) vesicles FRET efficiency was low (Fig. 8), as expected from the other experiments.

3.10. Quenching of W27 by Br_2-phosphatidylcholines

Whereas W27 was quenched significantly in SOPC membrane by all three brominated lipids, most efficient quencher was (9, 10)-Br_2-PC (Fig. 9). Similar quenching profiles were evident for POPG containing liposomes, however, the overall quenching efficiency was enhanced by the presence of the acidic phospholipid. Least effective quenching by brominated lipids was evident in the presence of liposomes containing both cholesterol and sphingomyelin (at $X=0.3$), again suggesting that LL-37 (F27W) was associated only weakly to the membrane surface. From the above data we calculated the penetration depth of Trp in bilayers by the parallax method [37] as well as distribution analysis [38,39] summarized in Table 3. These data confirm that the partitioning of the peptide into LUVs was strongly reduced by cholesterol and sphingomyelin and that the insertion of this peptide into the membrane was shallow.

4. Discussion

The aim of this study was to investigate the impact of different lipids on the interactions of LL-37 with monolayers, liposomes, and SLBs employed as model biomembranes. To better mimic the conditions prevailing *in vivo* unsaturated phospholipids were employed. In order to enable the use of fluorescence spectroscopy we constructed a mutant LL-37 with Phe27 replaced by Trp, this substitution chosen so as to have a minimal effect on the physicochemical characteristics of the peptide. The other three phenylalanines are flanked by cationic residues, which could in principle, quench the fluorescence of Trp. We also did not want to

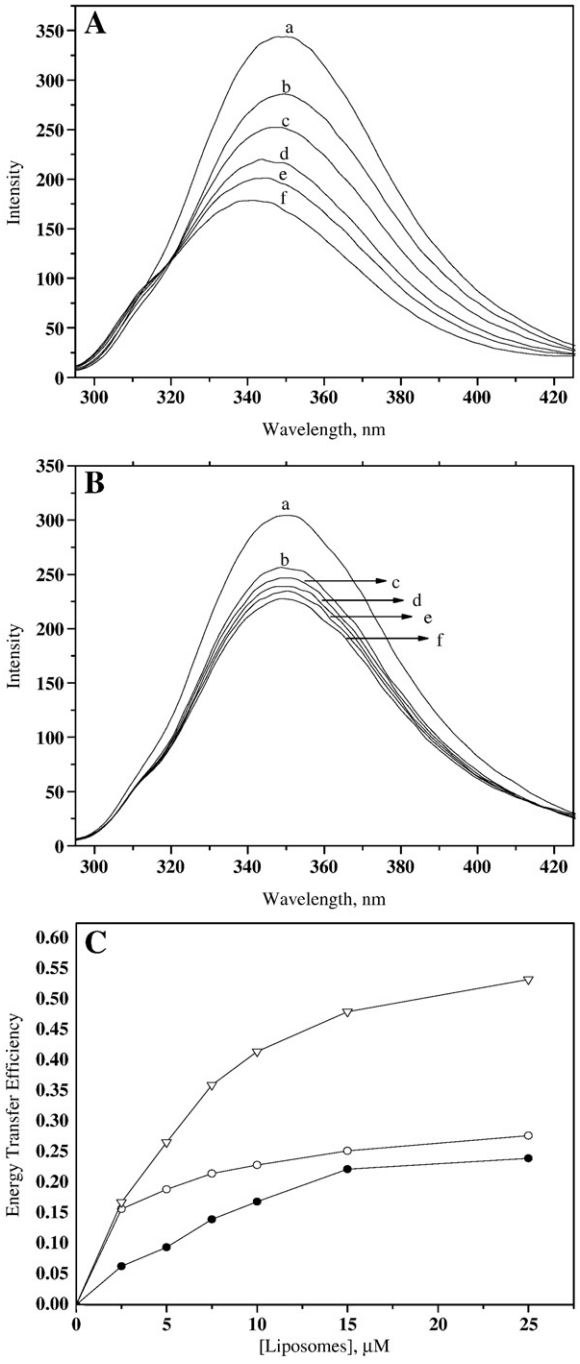

Fig. 8. *Panel A*: Emission spectra for LL-37(F27W) in the buffer (a) and in 2.5 (b), 5.0 (c), 7.5 (d), 10 (e), and 15 μM (f) of SOPC/POPG/DPPDns ($X_{POPG}=0.2$) liposomes. *Panel B*: Emission spectra for LL-37(F27W) in buffer (a) and in the presence of increasing concentrations of SOPC/Chol/Spm/DPPDns ($X_{Chol}=X_{Spm}=0.3$) liposomes as in *panel A*. *Panel C*: Energy transfer efficiency from Trp to dansyl as a function of liposome concentration for SOPC (○), SOPC with $X_{POPG}=0.2$ (▽), and SOPC with $X_{Chol}=X_{Spm}=0.3$ (●). The excitation wavelength was at 280 nm. The final concentration of LL-37(F27W) was 3 μM in a total volume of 2 mL of 5 mM Hepes, 0.1 mM EDTA, pH=7.0. The temperature was maintained at 25 °C with a circulating water bath.

have Trp-Phe (or Phe-Trp) in the sequence because of unpredictable impact of π–π interactions on Trp emission. Notably, the toxicity of LL-37 is not distinguished by Gram staining. Accordingly, at this stage we only tested the peptide against two Gram positive bacteria, *B. subtilis* and *S. aureus* and could confirm that both sensitivity and insensitivity to LL-37, respectively, of these microbes remained uninfluenced by the mutation W27F. Subsequent analysis of CD spectra further showed that the F27W mutant (Fig. 1) had essentially identical α-helical contents measured for native LL-37 both in the absence and presence of phospholipids, the latter increasing α-helicity [20]. Further characterization and comparison of the interaction of LL-37 and W27 mutant with lipids using monolayers and dynamic light scattering did reveal no significant differences, thus validating the F27W mutant as a model for LL-37.

A characteristic feature of cationic AMP's is that their association and insertion into bilayers is greatly augmented by the presence of negatively charged lipids. The latter constitute a major portion of the outer bacterial membranes and this preference is thought to underlie the differentiation by these peptides between the host and target cell membranes [21,26,43]. Our monolayer penetration measurements revealed that both LL-37 and LL-37 (F27W) intercalate equally effectively into both zwitterionic and negatively charged monolayers. Yet, DLS and fluorescence spectroscopy did reveal acidic phospholipids to promote the interaction of LL-37 with membranes. Major finding of the present study is that for membranes containing both cholesterol and sphingomyelin (at X=0.3) the membrane association of LL-37 and LL-37(F27W) is greatly reduced. This result was confirmed by fluorescence spectroscopy studies on the F27W peptide.

Eukaryotic plasma membranes are highly asymmetric with respect to the lipid composition of their outer and inner leaflets. More specifically, glycerophospholipids such as phosphatidylethanolamine and phosphatidylserine constitute a major fraction of the inner leaflet whereas sterols (cholesterol in mammals) and sphingolipids are enriched in the outer leaflet [48–50]. High

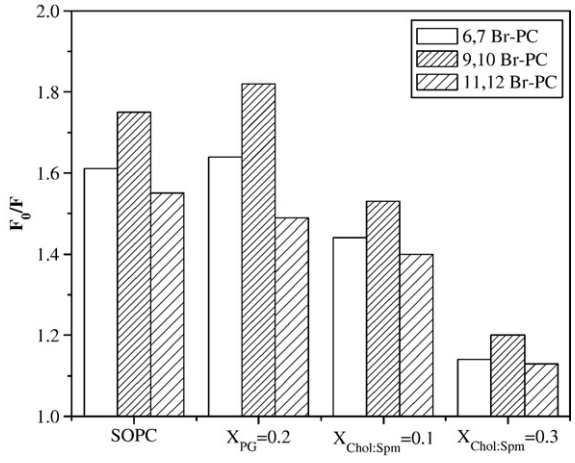

Fig. 9. Depth-dependent quenching of Trp fluorescence by SOPC liposomes containing brominated phosphatidylcholines (X=0.30) at a lipid/peptide molar ratio of 60. The concentration of LL-37(F27W) was 3 μM in a total volume of 2 mL of 5 mM Hepes, 0.1 mM EDTA, pH=7.0. The temperature was maintained at 25 °C with a circulating water bath. Each data point represents the mean of triplicate measurements.

Table 3
Penetration depth of Trp for the membrane bound LL-37(F27W) by distribution analysis and the parallax method

Lipid composition	Distance from the centre of the bilayer Z_{cF} (Å)	
	Distribution analysis	Parallax method
SOPC	9.65±0.9	10.68±1.3
X_{POPG}=0.2	9.56±1.2	10.20±1.5
$X_{Chol/Spm}$=0.3	10.0±1.5	10.98±1.9

[a]Depths were calculated from the fluorescence quenching obtained with samples containing brominated phosphatidylcholines (X=0.3). Samples were excited at 280 nm and emission was collected at 335 nm at L/P=100.

levels of sphingolipids and cholesterol have pronounced effects on the physical properties of lipid bilayers co-segregating into a distinct thermodynamic phase [51], the so-called liquid ordered (l_o) phase, different from both the solid ordered (s_o) and liquid disordered (l_d) phases [52–54]. Saturation is prevalent in sphingolipids, thus promoting the formation of the l_o phase. The rigid sterol ring augments *gauche→trans* isomerization of the lipid acyl chains and thus increases bilayer thickness, yet with little effect on the lateral diffusion of lipids in the plane of the bilayer. Cholesterol decreases the in-plane elasticity of PC and sphingomyelin monolayers [55] evident as high values for surface compression modulus. Consistent with our observations cholesterol at low mole fractions causes only a slight or no decrease in in-plane elasticity. However, $X_{Chol} \geq 0.2$ results in an abrupt reduction in the in-plane elasticity, in accordance with proximity to a critical point in the phase diagram [54,56] with conversion to l_o phase and thickening of the membrane. The l_o phase could be crucial in reducing the membrane association of LL-37 and thus protecting the host membranes from its membrane permeabilizing action, essential for the antimicrobial activity of this peptide.

Oren et al. used N-terminal fluorescently labeled LL-37 and FRET and concluded this peptide to oligomerize in the surface of phosphatidylcholine vesicles [21]. However, their FRET studies suggested that in the presence of negatively charged membranes LL-37 is monomeric. This may contradict our current findings showing the formation of amyloid-like fibrils by LL-37(F27W) to be induced by acidic phospholipids (Fig. 4). Yet, this difference could also result from the different peptide/lipid molar ratio used in these studies. In this context it could be relevant to note that because of poorly understood reasons FRET appears to be suppressed in "amyloid-like" fibrils [57]. We have recently reported on the formation of supramolecular protein-lipid fibers by several cytotoxic proteins and peptides, including some AMPs [29,32,42,43]. These fibers are macroscopic, with diameters of tens of microns, and yield upon staining with Congo red a light green birefringence, characteristic for amyloid. However, inspite of this staining by Congo red, to emphasize the fact that the fibers formed may not necessarily consist of extensive β-sheet structure, we have called these fibers "amyloid-like" [32]. As demonstrated by us for cytochrome *c*, the fibers may consist of protein trapped in different secondary structures, ranging from native-like conformation to extensive β-sheet [58]. Similarly to the other proteins and peptides studied so far the formation of amyloid-like fibrils by both LL-37 and LL-37(F27W) in the presence of liposomes containing negatively charged phospholipids is likely

to be driven by coulombic attraction between the cationic residues of the peptides and the anionic phospholipids, exhibiting no specificity with respect to the latter.

Fiber formation by LL-37 could be directly related to its cytotoxicity, similarly to the toxicity of fibrils formed by the paradigm of amyloid-forming peptides, Aβ, responsible for cell death and loss of tissue function in Alzheimer's disease [59]. There seems to be now consensus on the "mature" amyloid being inert and non-toxic to cells, while it is the early oligomeric states, protofibrils, which are toxic [60]. We have suggested this same mechanism to be responsible for both the pathological cytotoxicity of peptides such as Aβ, α-synuclein, and IAPP, as well as for the physiological cytotoxicity of some apoptotic proteins as well as antimicrobial peptides [31,42,43,61]. Mature amyloid fibers consist of extensively aggregated β-sheet structures, with the β-strands perpendicular to the fiber long axis [61], however, the structure of the toxic oligomers is not known. Their formation is preceded by aggregation, prompted by neutralization of their net cationic charge by acidic lipids [31]. We have suggested the "leaky slit" arrangement of the oligomers in membranes to fulfill the minimal requirement for the permeabilization of the target cell membrane [43]. Accordingly, the toxicity of this structure would not require any particular secondary structure, just the formation of a membrane inserted amphipathic oligomer with both hydrophobic and hydrophilic facets [43,52].

Induction of positive curvature strain into bilayers has been shown to be important for membrane disruption by cationic α-helical AMPs, as demonstrated for magainin 2 [1], temporins [33], and MSI-78 [62]. LL-37 disrupts the acyl chain packing and cooperativity of DMPC (zwitterionic) and DMPC/DMPG (anionic) bilayers and inserts into the hydrophilic/hydrophobic interface of the bilayer with the hydrophobic face of LL-37 helix extending approximately 5–6 Å from the surface into the hydrophobic acyl chain region of the bilayer [26]. The decreased access of the aqueous quencher acrylamide to Trp upon interaction of LL-37(F27W) with lipid vesicles should be accompanied by an increased accessibility to quenchers present in the hydrocarbon phase of the bilayers. Quenching with brominated lipids indicate that W27 resides at a distance of 9.65 to 9.56 Å from the center of the bilayer in the presence of zwitterionic and negatively charged membranes, locating in the shallow interfacial region near the headgroups of the lipids, as previously observed for Trps of several membrane embedded proteins and peptides [63,64]. Adsorption of the peptide on the membrane surface followed by its insertion into the hydrophobic phase and the presence of Trp, in the interfacial region supports the notion that the peptide first forms a local "carpet" on the membrane surface. Once a critical threshold concentration of the peptide is reached reorganization would then occur, leading to membrane disruption.

Membrane association of LL-37(F27W) was enhanced with net increasing negative surface charge density, irrespective of the acidic lipid headgroup, thus causing an augmented increase in $\Delta\lambda_{max}$ (Fig. 6, *panel A*). For SOPC the increase in $\Delta\lambda_{max}$ was attenuated until L/P ≤ 20 in keeping with the net charge of the membrane determining its interactions with the peptide. However, at L/P = 100 change in $\Delta\lambda_{max}$ is comparable to that seen for acidic liposomes, indicating that although electrostatic attraction increases the affinity of the peptide to the membrane, also hydrophobicity driven binding of the peptide to the membrane is significant. The decrease in I at L/P ≤ 10 could be attributed to LL-37 existing as oligomers even at micromolar concentrations. Accordingly, it could be in an aggregated state also upon binding to SOPC LUVs as well as on the surface of cholesterol/sphingomyelin containing membranes. In the aggregated state the Trp residues may be in close proximity to each other thus resulting in self-quenching. Likewise, quenching could be caused by proximity of Trp to positive charges of the peptide, as suggested for nisin and temporin L [48]. Yet, also the charged headgroup of POPG may interact directly with the π-orbitals of Trp [48].

Increase of ζ and d_Z upon the addition of LL-37 to SOPC and SOPC/cholesterol (X_{Chol} = 0.1) liposomes is in accordance with a gradual accumulation of the peptide onto the membrane. The value for ζ becomes constant at P/L = 0.006 suggesting that peptide has saturated the membrane surface. However, at higher peptide concentration d_Z still decreases, perhaps indicating penetration of peptide into the bilayer. In the presence of cholesterol (X_{Chol} = 0.1) higher surface contents of the peptide (P/L = 0.01) are needed for d_Z to decrease, indicating diminished affinity of the peptide to this membrane. The continuous increase in d_Z at all P/L ratios for liposomes containing $X_{Chol} = X_{Spm} = 0.3$ is likely to indicate that peptide accommodates only on the surface of the bilayer, in accordance with the least changes in $\Delta\lambda_{max}$ and effective quenching of Trp emission by acrylamide. Decrement in d_Z in the presence of acidic phospholipids at all P/L ratios by LL-37 and LL-37(F27W) could be due to partial solubilization of liposomes by the peptides. This behavior may be attributed to strong electrostatic interactions at low peptide concentrations between their positive charges and negatively charged lipid headgroup, resulting in peptide aggregation and insertion into the bilayer. Interestingly, a sharp increase in d_Z was observed at P/L = 0.1 (data not shown) in the presence of SOPC/POPG (X_{POPG} = 0.2) LUVs. This increase could be due to *(i)* vesicle aggregation due to high peptide concentration, *(ii)* fragmentation of the bilayer via carpet like mechanism, or *(iii)* formation of amyloid-like fibers. The above processes could occur on negatively charged membranes depending on the local peptide concentration, as is evident from spectroscopic and microscopic observations. In DLS measurements the size of the particles in aqueous solution is derived from the translational diffusion coefficient of one particle, reflected in the fluctuation of scattered light intensity. The diffusion of fibrils should be slow. Accordingly, the size of the fibrillar assembly would appear to be very large.

Supported lipid bilayers represent an interesting model biomembrane to assess the impact of AMPs on the 2- and 3-D organization of the resulting supramolecular assemblies [33]. Application of LL-37 and LL-37(F27W) at L/P ≈ 2:1 on SLBs containing negatively charged lipids caused the generation of multilamellar and unilamellar vesicles, resulting in the disintegration and rearrangement of the supported bilayer. This suggests that at high L/P ratios peptide may accumulate in the lipid bilayer surface, partially penetrating into the hydrophobic region, accompanying the reduction of the surface charge due to electrostatic peptide–lipid interactions. However, at lower L/P the surface charge of the outer leaflet in bilayers is reduced or

neutralized by the cationic groups of peptide, facilitating interactions with other liposomes through charge interaction. The reduction in surface charge may lead to a decrease in the ability of peptides to attach to the lipid bilayer. As a result, the predominant hydrophobic interaction between the peptide and lipids would favor the penetration of LL-37 into the nonpolar acyl chain region, perturbing the membrane and causing fusion, so as to lead to the generation of unilamellar and multilamellar vesicles from the supported bilayer. Interestingly, Hertog et al. [65] observed that the association of LL-37 to the cell wall and plasma membrane of *Candida albicans*, is accompanied by extensive disintegration of the membrane into vesicle-like structures and leakage of vital cellular components, including ATP. They also found LL-37 to induce phase separation in the membrane, irrespective of its efficiency of transmigration of membrane [65].

Our results with LL-37 (at 3 μM concentration, which is within the MIC of this peptide) and model biomembranes using different biophysical techniques reveal that although LL-37 is effective in perturbing both zwitterionic (SOPC) as well as mixed membranes containing the negatively charged POPG the extent of membrane interactions of LL-37 are augmented in the presence of latter phospholipid as evident from the larger shift in λ_{max}, higher $\Delta\pi$, more efficient energy transfer, augmented quenching by brominated phospholipids, higher α-helical content, decrease in d_Z, formation of amyloid-like fibers, and generation of multilamellar and unilamellar vesicles from SLBs. No differences in the binding of LL-37(F27W) to POPG and POPS were evident thus corroborating the idea that electrostatic interactions between the positively charged LL-37(F27W) and negatively charged headgroups of POPG/POPS changes the way peptide resides in the membrane and alters its aggregation state. The penetration depth of the Trp residue is unlikely to depend on the acidic lipid headgroup because the blue shift of fluorescence emission was the same for both POPG and POPS containing bilayers. The secondary structure of the peptide was also independent of these lipid species (Fig. 1). Interestingly, membranes containing both cholesterol and sphingomyelin (both at $X=0.3$) were highly effective in attenuating the membrane binding of LL-37. Accordingly, the distinction between target and host cells by LL-37 is likely to derive from both enhanced association with the former cells caused by acidic phospholipids as well as from attenuated interactions with the outer surface of the plasma membrane of the peptide secreting host, imposed by its high content of cholesterol and sphingomyelin.

Acknowledgments

The authors thank Kristiina Soderholm and Kaija Niva for their technical assistance. HBBG is supported by the Finnish Academy, Sigrid Juselius Foundation, and Marie Curie Incoming International Fellowship from European Commission (Y.D.).

References

[1] K. Matsuzaki, K. Sugishita, N. Ishibe, M. Ueha, S. Nakata, K. Miyajima, R.M. Epand, Relationship of membrane curvature to the formation of pores by magainin 2, Biochemistry 37 (1998) 11856–11863.

[2] D. Yang, O. Chertov, J.J. Oppenheim, Participation of mammalian defensins and cathelicidins in anti-microbial immunity: receptors and activities of human defensins and cathelicidins (LL-37), J. Leukoc. Biol. 69 (2001) 691–697.

[3] M. Zanetti, R. Gennaro, D. Romeo, Cathelicidins: a novel protein family with a common proregion and a variable C-terminal antimicrobial domain, FEBS Lett. 374 (1995) 1–5.

[4] B. Agerberth, J. Charo, J. Werr, B. Olsson, F. Idali, L. Lindbom, R. Kiessling, H. Jornvall, H. Wigzell, G.H. Gudmundsson, The human antimicrobial and chemotactic peptides LL-37 and alpha-defensins are expressed by specific lymphocyte and monocyte populations, Blood 96 (2000) 3086–3093.

[5] M. Zanetti, G.D. Sal, P. Storici, C. Schneider, D. Romeo, The cDNA of the neutrophil antibiotic Bac5 predicts a pro-sequence homologous to a cysteine proteinase inhibitor that is common to other neutrophil antibiotics, J. Biol. Chem. 268 (1993) 522–526.

[6] A. Ritonja, M. Kopitar, R. Jerala, V. Turk, Primary structure of a new cysteine proteinase inhibitor from pig leukocytes, FEBS Lett. 255 (1989) 211–214.

[7] M. Kopitar, A. Ritonja, T. Popovic, D. Gabrijelcic, A new type of low-molecular mass cysteine proteinase inhibitor from pig leukocytes, Biol. Chem. Hoppe-Seyler. 370 (1989) 1145–1151.

[8] B. Agerberth, H. Gunne, H. Odeberg, P. Kogner, H.G. Boman, G.H. Gudmundsson, FALL-39, a putative human peptide antibiotic, is cysteine-free and expressed in bone marrow and testis, Proc. Natl. Acad. Sci. U. S. A. 92 (1995) 195–199.

[9] J.W. Larrick, M. Hirata, R.F. Balint, J. Lee, J. Zhong, S.C. Wright, Human CAP 18: a novel antimicrobial lipopolysaccharide-binding protein, Infect. Immun. 63 (1995) 1291–1297.

[10] J.B. Cowland, A.H. Johnsen, N. Borregaard, hCAP-18, a cathelin/pro-bactenecin-like protein of human neutrophil specific granules, FEBS Lett. 368 (1995) 173–176.

[11] H. Gudmundsson, B. Agerberth, J. Odeberg, T. Bergman, B. Olsson, R. Salcedo, The human gene FALL39 and processing of the cathelin precursor to the antibacterial peptide LL-37 in granulocytes, Eur. J. Biochem. 238 (1996) 325–332.

[12] O. Sorensen, K. Arnljots, J.B. Cowland, D.F. Bainton, N. Borregaard, The human antibacterial cathelicidin, hCAP-18, is synthesized in myelocytes and metamyelocytes and localized to specific granules in neutrophils, Blood 90 (1997) 2796–2803.

[13] M. Frohm, B. Agerberth, G. Ahangari, M.S. Backdahl, S. Liden, H. Wigzell, G.H. Gudmundsson, The expression of the gene coding for the antibacterial peptide LL-37 is induced in human keratinocytes during inflammatory disorders, J. Biol. Chem. 272 (1997) 15258–15263.

[14] D. Tanaka, K.Y. Miyasaki, R.I. Lehrer, Sensitivity of *Actinobacillus actinomycetemcomitans* and *Capnocytophaga* spp. to the bactericidal action of LL-37: a cathelicidin found in human leukocytes and epithelium, Oral Microbiol. Immunol. 15 (2000) 226–231.

[15] J.W. Larrick, M. Hirata, J. Zhong, S.C. Wright, Anti-microbial activity of human CAP18 peptides, Immunotechnology 1 (1995) 65–72.

[16] J.Y. Moon, K.A.H. Wildman, A. Ramamoorthy, Expression and purification of a recombinant LL-37 from *Escherichia coli*, Biochim. Biophys. Acta 1758 (2006) 1351–1358.

[17] R. Bals, D.J. Weiner, A.D. Moscioni, R.L. Meegalla, J.M. Wilson, Augmentation of innate host defense by expression of a cathelicidin antimicrobial peptide, Infect. Immun. 67 (1999) 6084–6089.

[18] J. Malm, O. Sorenson, T. Peterson, The human cationic antimicrobial protein (hCAP-18) is expressed in the epithelium of human epididymis, is present in the seminal plasma at high concentrations, and is attached to spermatozoa, Infect. Immun. 68 (2000) 4297–4302.

[19] K. Hase, L. Eckmann, J.D. Leopard, N. Varki, M.F. Kagnoff, Cell differentiation is a key determinant of cathelicidin LL-37 /human cationic antimicrobial protein 18 expression by human colon epithelium, Infect. Immun. 70 (2002) 953–963.

[20] J. Johansson, G.H. Gudmundson, M.E. Rottenberg, K.D. Berndt, B. Agerberth, Conformation-dependent antibacterial activity of the naturally occurring human peptide LL-37, J. Biol. Chem. 273 (1998) 3718–3724.

[21] Z. Oren, J.C. Lerman, G.H. Gudmundsson, B. Agerberth, Y. Shai, Structure and organization of the human antimicrobial peptide LL-37 in

phospholipid membranes: relevance to the molecular basis for its non cell selective activity, Biochem. J. 341 (1999) 501–513.
[22] O. Sorenson, T. Bratt, A.H. Johnsen, M.T. Madsen, N. Borregaard, The human antibacterial cathelicidin, hCAP-18, is bound to lipoproteins in plasma, J. Biol. Chem. 274 (1999) 22445–22451.
[23] Y. Wang, B. Agerberth, A. Lothgren, A. Almstedt, J. Johansson, Apolipoprotein A-I binds and inhibits the human antibacterial/cytotoxic peptide LL-37, J. Biol. Chem. 273 (1998) 33115–33118.
[24] U.H.N. Durr, U.S. Sudheendra, A. Ramamoorthy, LL-37, the only human member of the cathelicidin family of antimicrobial peptides, Biochim. Biophys. Acta 1758 (2006) 1408–1425.
[25] F. Neville, M. Cahuzac, O. Konovalov, Y. Ishitsuka, K.Y.C. Lee, I. Kuzmenko, G.M. Kale, D. Gidalevitz, Lipid headgroup discrimination by antimicrobial peptide LL-37: Insight into mechanism of action, Biophys. J. 90 (2006) 1275–1287.
[26] K.A.H. Wildman, D.K. Lee, A. Ramamoorthy, Mechanism of lipid bilayer disruption by the human antimicrobial peptide, LL-37, Biochemistry 42 (2003) 6545–6558.
[27] F. Neville, M. Cahuzac, A. Nelson, D. Gidalevitz, The interaction of antimicrobial peptide LL-37 with artificial biomembranes: epifluorescence and impedence spectroscopy approach, J. Phys., Condens. Matter 16 (2004) S2413–S2420.
[28] K.A.H. Wildman, G.V. Martinez, M.F. Brown, A. Ramamoorthy, Perturbation of the hydrophobic core of lipid bilayers by the human antimicrobial peptide LL-37, Biochemistry 43 (2004) 8459–8469.
[29] R. Sood, Y. Domanov, P.K.J. Kinnunen, Fluorescent temporin B derivative and its binding to liposomes, J. Fluoresc. 17 (2007) 223–234.
[30] L.S. Bernstein, A.A. Grillo, S.S. Loranger, M.E. Linder, RGS4 binds to membranes through an amphipathic α-helix, J. Biol. Chem. 275 (2000) 18520–18526.
[31] H. Zhao, J.P. Mattila, J.M. Holopainen, P.K.J. Kinnunen, Comparison of the membrane association of two antimicrobial peptides, magainin 2 and indolicidin, Biophys. J. 81 (2001) 2979–2991.
[32] H. Zhao, E.K.J. Tuominen, P.K.J. Kinnunen, Formation of amyloid fibers triggered by phosphatidylserine-containing membranes, Biochemistry 43 (2004) 10302–10307.
[33] Y.A. Domanov, P.K.J. Kinnunen, Antimicobial peptides temporins B and L induce formation of tubular lipid protrusions from supported phospholipid bilayers, Biophys. J. 91 (2006) 4427–4439.
[34] K. Zhu, A. Jutila, E.K.J. Tuominen, P.K.J. Kinnunen, Effects of i-propanol on the structural dynamics of thermomyces lanuginosa lipase revealed by tryptophan fluorescence, Protein Sci. 10 (2001) 339–351.
[35] A.I.P.M.D. Karoon, M.W. Soekarjo, J.D. Gier, B.D. Kruijff, The role of charge and hydrophobicity in peptide–lipid interaction: a comparative study based on tryptophan fluorescence measurements combined with the use of aqueous and hydrophobic quenchers, Biochemistry 29 (1990) 8229–8240.
[36] M.R. Eftink, C.A. Ghiron, Fluorescence quenching of indole and model micelle systems, J. Phys. Chem. 80 (1976) 486–493.
[37] A. Chattopadhyay, E. London, Parallax method for direct measurement of membrane penetration depth utilizing fluorescence quenching by spin-labeled phospholipids, Biochemistry 26 (1987) 39–45.
[38] A.S. Ladokhin, P.W. Holloway, E.G. Kostrzhevska, Distribution analysis of membrane penetration of proteins by depth-dependent fluorescence quenching, J. Fluoresc. 3 (1993) 195–197.
[39] A.S. Ladokhin, Analysis of protein and peptide penetration into membranes by depth-dependent fluorescence quenching: theoretical considerations, Biophys. J. 76 (1999) 946–955.
[40] D. Marsh, Lateral pressure in membranes, Biochim. Biophys. Acta 1286 (1996) 183–223.
[41] T. Söderlund, J.M. Alakoskela, A.L. Pakkanen, P.K.J. Kinnunen, Comparison of the effects of surface tension and osmotic pressure on the interfacial hydration of a fluid phospholipid bilayer, Biophys. J. 85 (2003) 2333–2341.
[42] H. Zhao, A. Jutila, T. Nurminen, S.A. Wickstrom, J. Keski-Oja, P.K.J. Kinnunen, Binding of endostatin to phosphatidylserine-containing membranes and formation of amyloid like fibers, Biochemistry 44 (2005) 2857–2863.
[43] H. Zhao, R. Sood, A. Jutila, S. Bose, G. Fimland, J.N. Meyer, P.K.J. Kinnunen, Interaction of the antimicrobial peptide pheromone Plantaricin A with model membranes: implications for a novel mechanism of action, Biochim. Biophys. Acta 1758 (2006) 1461–1474.
[44] J.R. Lakowicz, Principles of Fluorescence Spectroscopy, Plenum Press, 1999, p. New York.
[45] E.P. Kirpy, R.F. Steiner, Influence of solvent and temperature upon the fluorescence of indole derivatives, J. Phys. Chem. 74 (1970) 4480–4490.
[46] A.J. Weaver, M.D. Kemple, J.W. Brauner, R. Mendelsohn, F.G. Prendergast, Fluorescence, CD, attenuated total reflectance (ATR) FTIR, and carbon-13 NMR characterization of the structure and dynamics of synthetic melittin and melittin analogs in lipid environments, Biochemistry 31 (1992) 1301–1313.
[47] D.A. Dougherty, Cation–π interactions in chemistry and biology: a new view of benzene, Phe, Tyr, and Trp, Science 271 (1996) 163–167.
[48] H. Zhao, P.K.J. Kinnunen, Binding of antimicrobial peptide temporin L to liposomes assessed by Trp fluorescence, J. Biol. Chem. 277 (2002) 25170–25177.
[49] E.M. Tytler, G.M. Anantharamaiah, D.E. Walker, V.K. Mishra, M.N. Palgunachari, J.P. Segrest, Molecular basis for prokaryotic specificity of magainin-induced lysis, Biochemistry 34 (1995) 4293–4401.
[50] P.A. Janmey, P.K.J. Kinnunen, Biophysical properties of lipids and dynamic membranes, Trends Cell Biol. 16 (2006) 538–546.
[51] M.B. Sankaram, T.E. Thompson, Interaction of cholesterol with various glycerophospholipids and sphingomyelin, Biochemistry 29 (1990) 10670–10675.
[52] J.H. Ipsen, G. Karlström, O.G. Mouritsen, H. Wennerström, M.J. Zuckermann, Phase equilibria in the phosphatidylcholine–cholesterol system, Biochim. Biophys. Acta 905 (1987) 162–172.
[53] M.R. Vist, J.H. Davis, Phase equilibria of cholesterol/dipalmitoylphosphatidylcholine mixtures: deuterium nuclear magnetic resonance and differential scanning calorimetry, Biochemistry 29 (1990) 451–464.
[54] B.M. Castro, R.F.M. de Almeida, L.C. Silva, A. Fedorov, M. Prieto, Formation of ceramide/sphingomyelin gel domains in the presence of an unsaturated phospholipid: a quantitative multiprobe approach, Biophys. J. 93 (2007) 1639–1650.
[55] X.M. Li, M.M. Momsen, J.M. Smaby, H.L. Brockman, R.E. Brown, Cholesterol decreases the interfacial elasticity and detergent solubility of sphingomyelins, Biochemistry 40 (2001) 5954–5963.
[56] M.B. Sankaram, T.E. Thompson, Cholesterol-induced fluid-phase immiscibility in membranes, Proc. Natl. Acad. Sci. U. S. A. 88 (1991) 8686–8690.
[57] J. Kaylor, N. Bodner, S. Edridge, G. Yamin, D.P. Hong, A.L. Fink, Characterization of oligomeric intermediates in α-synuclein fibrillation: FRET studies of Y125W/Y133F/Y136F α-synuclein, J. Mol. Biol. 353 (2005) 357–372.
[58] J.M. Alakoskela, A. Jutila, A.C. Simonsen, J. Pirneskoski, S. Pyhajoki, R. Turunen, S. Marttila, O.G. Mouritsen, E. Goormaghtigh, P.K.J. Kinnunen, Characteristics of fibers formed by cytochrome *c* and induced by anionic phospholipids, Biochemistry 45 (2006) 13447–13453.
[59] M.R.R. Planque, V. Raussens, S.A. Contera, D.T.S. Rijkers, R.M.J. Liskamp, J.M. Ruysschaert, J.F. Ryan, F. Separovic, A. Watts, β-sheet structured β-amyloid(1-40) perturbs phosphatidylcholine model membranes, J. Mol. Biol. 368 (2007) 982–997.
[60] B. Caughey, P.T. Lansbury, Protofibrils, pores, fibrils, and neurodegeneration: separating the responsible protein aggregates from the innocent bystanders, Annu. Rev. Neurosci. 26 (2003) 267–298.
[61] G.P. Gorbenko, P.K.J. Kinnunen, The role of lipid–protein interactions in amyloid-type protein fibril formation, Chem. Phys. Lipids 141 (2006) 72–82.
[62] K.J. Hallock, D.K. Lee, A. Ramamoorthy, MSI-78, an analogue of the magainin antimicrobial peptides, disrupts lipid bilayer structure via positive curvature strain, Biophys. J. 84 (2003) 3052–3060.
[63] K. Matsuzaki, O. Murase, H. Tokuda, S. Funakoshi, N. Fujii, K. Miyajima, Orientational and aggregational states of magainin 2 in phospholipid bilayers, Biochemistry 33 (1994) 3342–3349.
[64] S.H. White, W.C. Wimley, Peptides in lipid bilayers: structural and thermodynamic basis for partitioning and folding, Curr. Opin. Struct. Biol. 4 (1994) 79–86.
[65] A.L. Hertog, J.V. Marle, E.C. Veerman, M.B. Valentijin, K. Nazmi, H. Kalay, C.H. Grun, W. Van't Hof, J.G. Bolscher, A.V.N. Amerongen, The human cathelicidin peptide LL-37 and truncated variants induce segregation of lipids and proteins in the plasma membrane of *Candida albicans*, Biol. Chem. 387 (2006) 1495–1502.